Journal of Organometallic Chemistry, 200 (1980) 37—61
Elsevier Sequoia S.A., Lausanne — Printed in The Netherlands

LARGE METAL CARBONYL CLUSTERS (LMCC)

(the late) P. CHINI
Istituto di Chimica generale dell'Università, Via G. Venezian 21, 20133 Milano (Italy)

Table of contents

Introduction

This work originated in 1958 when trying to repeat a patent [44] which claimed that a mixture of iron and cobalt carbonyls gave improved selectivity in hydroformylation: an unusual wine-red coloured solution was obtained, from which was isolated the first mixed metal carbonyl, the violet $HFeCo_3(CO)_{12}$ [24,25]. However, the real introduction to high nuclearity clusters [27] came about six months later when attempting to produce mixed cobalt-chromium species by heating a mixture of $Co_2(CO)_8$ and $Cr(CO)_6$. An unusual deep-green solution was obtained, which gave a green precipitate on addition of dilute ammonia and this solid surprisingly did not contain chromium. Unfortunately, this problem had to wait until December 1965, when it became possible to tackle it again at the Institute of General and Inorganic Chemistry of the University of Milano *. After some effort a green caesium salt was separated from the accompanying $Cs[Co(CO)_4]$ by precipitation from water. Once the formula $Cs_2[Co_6(CO)_{15}]$ was determined (March 1966), we became interested

---

* I am obliged to Prof. L. Malatesta for giving me this opportunity.

in the reactions of the isoelectronic hexanuclear cluster, $Rh_6(CO)_{16}$, and a host of new clusters was rapidly isolated [84].

The entry into the platinum field [60] originated from a NATO fellowship, spent in Brighton (England) working with Joe Chatt, and from the puzzling observation reported by Booth and Chatt [15] that "dicarbonylplatinum" dissolves in acetone in the presence of aqueous ammonia to give a dark green solution. Finally, because of the difficulties encountered in the platinum work, we hoped that we could make useful IR comparisons with the "known" nickel carbonyl anionic clusters [47] and thus we entered the nickel field [35].

Therefore between 1967 and 1968 we already had definite IR and chemical evidence that a very extensive, and previously ignored, chemistry of high nuclearity clusters of Co, Rh, Ni and Pt was at hand, although only a few of them had been structurally characterised at that time.

Apart from curiosity, which has always been the main driving force, in 1965 the original aim of the work was to provide evidence for the existence of cobalt species deficient in carbon monoxide which could explain the large change in rate and product distribution observed in hydroformylation at low partial pressures of carbon monoxide [81,82]. Later on (1968) I concluded a review article in this way: "Polycentric ligand—metal bonds and delocalised metal—metal bonds are probably common features of closed metal carbonyl clusters and of molecules chemisorbed on metal surfaces; the importance of closed metal carbonyl clusters as models for catalytic reactions on metal surfaces is emerging at present" [26]. Today we can add that large metal carbonyl clusters have provided information relevant to solid state chemistry and therefore, as originally pointed out many years ago by Schafer and Schnering in the case of halide clusters [87], represent a further area bridging solid state and coordination chemistry.

Synthesis of LMCC

There are three general methods presently available for the synthesis of large carbonyl clusters: oxidative coupling, redox condensation and thermal condensation. Photochemical condensation is very promising, but has not yet been properly exploited. When suitable reagents are available, redox condensation allows a step by step growth of the cluster and generally may be controlled to give nearly quantitative yields. On the contrary, control of thermal condensation is more limited and low yields sometimes result.

The first example of redox condensation was reported by Hieber and Schubert in 1965 [48]:

$$[Fe_3(CO)_{11}]^{2-} + Fe(CO)_5 \xrightarrow[THF]{25^\circ C} [Fe_4(CO)_{13}]^{2-} + 3\ CO \qquad (1)$$

It seems probable that, in this case, the first step is a redox transfer giving rise to radical anions such as $[Fe_3(CO)_{11}]^-$ and $[Fe(CO)_5]^-$ [55], once formed these are highly reactive species and a condensation may follow. One driving force for the condensation is the spread of the negative charge over a larger number of metal atoms and the associated increase in average back-donation to the ligands. This is the case with simple redox redistribution reactions in which both the number of metal—metal and metal—ligand bonds remains constant. For instance [61]:

$$[Pt_6(CO)_{12}]^{2-} + [Pt_{12}(CO)_{24}]^{2-} \xrightarrow[\text{THF}]{25^\circ\text{C}} 2[Pt_9(CO)_{18}]^{2-} \tag{2}$$

However, in many condensations carbon monoxide is usually evolved and new metal—metal bonds are formed. The following reactions, which are reversed at —70°C [70,42],

$$[Rh_5(CO)_{15}]^- + [Rh(CO)_4]^- \underset{-70^\circ\text{C, THF, 1 atm CO}}{\overset{25^\circ\text{C, THF, 1 atm CO}}{\rightleftharpoons}} [Rh_6(CO)_{15}]^{2-} + 4\ CO \tag{3}$$

$$[Rh_6(CO)_{15}]^{2-} + [Rh(CO)_4]^- \underset{-70^\circ\text{C, MeOH, 1 atm CO}}{\overset{25^\circ\text{C, MeOH, 1 atm CO}}{\rightleftharpoons}} [Rh_7(CO)_{16}]^{3-} + 3\ CO \tag{4}$$

show clearly that redox condensations are endothermic processes ($\bar{D}$(M—CO) ~ 35—45 and $\bar{D}$(M—M) ~ 20—30 kcal mol^{-1}) [34] which are readily balanced on increasing the temperature due to the large increase in entropy from the formation of gaseous carbon monoxide ($T\Delta S$ ~ 7—8 kcal mol^{-1} of evolved CO).

Redox condensation is more favoured with second and third row transition elements in agreement with a decrease in the difference between $\bar{D}$(M—CO) and $\bar{D}$(M—M) on descending the subgroups [27]. Moreover, when both species involved in the redox condensation contain a high negative charge, the high value of the bonding energy, $\bar{D}$(M—CO), opposes the condensation. As a result highly reduced species are increasingly difficult to prepare and generally sensitive to demolition by carbon monoxide [27].

The step by step growth, which is possible using redox condensation processes, is clearly illustrated by reaction 5 followed by reactions 3 and 4 [42]:

$$Rh_4(CO)_{12} + [Rh(CO)_4]^- \xrightarrow[\text{1 atm CO}]{25^\circ\text{C, THF}} [Rh_5(CO)_{15}]^- + CO \tag{5}$$

A further recent example is the following sequence which, on the contrary, results in the capping of square faces [74a]:

$$[Rh_{13}(CO)_{24}H]^{4-} + [Rh(CO)_2(CH_3CN)_2]^+ \xrightarrow[CH_3CN]{25^\circ\text{C}} [Rh_{14}(CO)_{25}H]^{3-} + CO \tag{6}$$

$$[Rh_{14}(CO)_{25}H]^{3-} \xrightarrow{Na_2CO_3} [Rh_{14}(CO)_{25}]^{4-} \tag{7}$$

$$[Rh_{14}(CO)_{25}]^{4-} + [Rh(CO)_2(CH_3CN)_2]^+ \xrightarrow[CH_3CN]{25^\circ\text{C}} [Rh_{15}(CO)_{27}]^{3-} \tag{8}$$

Although the two capping processes are nearly equivalent, both electronically (usually 12 el.) and in terms of space filling increase (17.6% for triangular capping and 19.7% for square capping), they are considerably different in terms of the number of new coordination positions available to the carbonyl ligands (~3 for triangular capping and ~2 for square capping).

Although thermal condensation of preformed clusters offers unlimited synthetic possibilities it requires a time-consuming and careful screening of the experimental conditions, because the composition of the reaction mixture is extremely dependent even on minor experimental changes. Moreover the availability of a simple process for the separation of the reaction mixture is generally crucial. Recent examples of this method are [7,23,74a]:

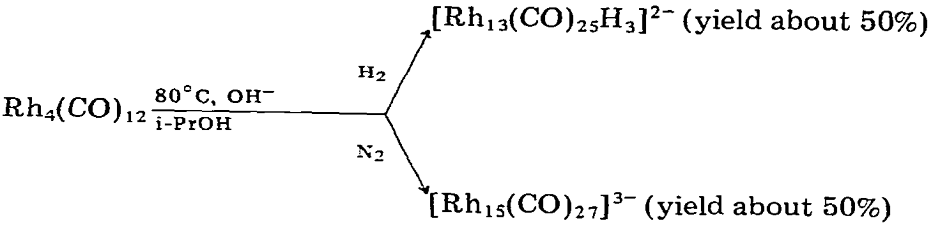

$$Rh_4(CO)_{12} \xrightarrow[\text{i-PrOH}]{80^\circ C,\ OH^-} \begin{cases} \xrightarrow{H_2} [Rh_{13}(CO)_{25}H_3]^{2-} \text{ (yield about 50\%)} \\ \xrightarrow{N_2} [Rh_{15}(CO)_{27}]^{3-} \text{ (yield about 50\%)} \end{cases} \tag{9}$$

$$5[Pt_9(CO)_{18}]^{2-} + [Pt_{12}(CO)_{24}]^{2-} \xrightarrow[\left\{\begin{array}{c}30\ \text{min. at } 50^\circ C \\ + \\ 30\ \text{min. at } 80^\circ C\end{array}\right.]{CH_3CN} 3[Pt_{19}(CO)_{22}]^{4-} + 48\ CO \quad \text{(yield about 80\%)} \tag{10}$$

Oxidative coupling of anionic species has been used for many years for obtaining large rhodium carbide clusters by oxidation of the $[Rh_6(CO)_{15}C]^{2-}$ dianion with iron(III) salts [27]. A cleaner coupling is often observed when protonation gives rise to unstable hydride derivatives; for instance [17,90]:

$$2[Ni_6(CO)_{12}]^{2-} + 2\ H^+ \xrightarrow[H_2O]{pH\ 4} [Ni_{12}(CO)_{21}H_2]^{2-} + 3\ CO \tag{11}$$

(yield about 90%)

$$2[Rh_6(CO)_{15}C]^{2-} + 2\ H^+ \rightarrow [Rh_{12}(CO)_{24}(C)_2]^{2-} + 6\ CO + H_2 \tag{12}$$

Finally our entry into the chemistry of carbides resulted from the fortuitous presence of chloroform when carrying out the direct reduction of Rh^{III} salts [27]·

$$6[RhCl_6]^{3-} + 23\ OH^- + 26\ CO + CHCl_3 \xrightarrow[MeOH]{25^\circ C,\ 1\ atm\ CO} [Rh_6(CO)_{15}C]^{2-} + 39\ Cl^- + 11\ CO_2 + 12\ H_2O \tag{13}$$

The carbide chemistry was readily extended to cobalt by starting from preformed $Co_3(CO)_9CCl$, although attempts to obtain similar carbide clusters of platinum and iridium have as yet failed.

Comparison of LMCC and metallic lattices

The tetrahedron and the octahedron are subunits common to both the hexagonal and the cubic close packed lattices. They are also the more common arrangements of metal atoms found in tridimensional clusters, a fact which probably led to the belief that clusters are finite pieces of giant metallic lattices. However, the situation is not so simple: similarities between metals and clusters arise because of the same necessity to maximise the number of metallic interactions in order to provide maximum bonding energy. Differences also arise because in finite clusters the constraint imposed by the periodic repetition required in an infinite lattice is absent, and considerable freedom

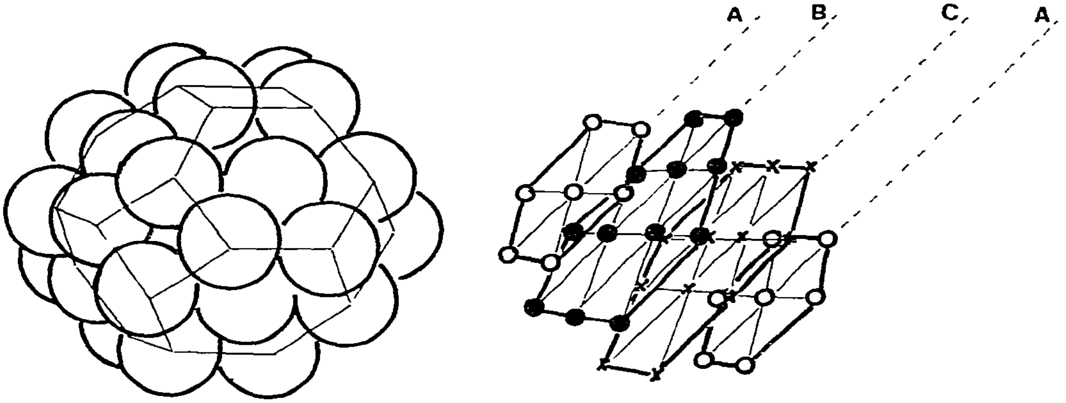

Fig. 1. The truncated octahedron of platinum atoms (O_h) found in the $[Pt_{38}(CO)_{44?}]^{2-}$ cluster [23], and the sequence of ccp layers.

of arrangement around a central metal atom is allowed [31]. Moreover, as we will discuss later, clusters require large surfaces able to accommodate the ligands without excessive steric crowding.

Only one large cluster having a ccp arrangement of metal atoms has yet been structurally characterised, although, owing to the technical problem of locating the small carbonyls in the presence of 38 platinum atoms, the number of ligands and their distribution have not yet been determined. Chemical analysis indicates the presence of about 44 ligands, in agreement with the theoretical prediction of J. Lauher [58], however, with our present level of knowledge the possible presence of hydride ligands cannot be discounted. Fig. 1 shows the regular truncated octahedron of platinum atoms which has been found in this fragment of platinum metal (ccp). There are 144 Pt—Pt bonds of average value 2.83 Å (2.77 Å in the metal), and the diameter of the metallic skeleton is 11.6 Å. The more unexpected property of the salts of this cluster (for instance PPN^+) is that they are well soluble in organic solvents such as THF, CH_2Cl_2 and acetone. The carbonyl stretching frequencies are of particular interest because of their possible resemblance to those of carbon monoxide chemisorbed on platinum; unfortunately they occur at lower frequencies (2050 and 1807 cm^{-1} in THF) [23] due to the presence of the negative charge [27].

Our knowledge of the cluster $[Pt_{26}(CO)_{32}]^{2-}$ is better because in this case it has been possible to locate the carbonyl ligands [23]. It is quite interesting that the arrangements of the platinum atoms shown in Fig. 2 is now hcp; probably as in the case for finite lattices, the difference in energy of the different packings of metal atoms could be small enough to resist interpretation. There are other clusters in which there is a clear correspondence with the hcp lattice. Fig. 3 shows the regular twinned cube-octahedron found in the three $[Rh_{13}(CO)_{24}H_{5-n}]^{n-}$ species ($n = 2, 3, 4$) [7,8,74a], whereas Fig. 4 shows the truncated trigonal bipyramid found in the three structurally characterised $[Ni_{12}(CO)_{21}H_{4-n}]^{n-}$ species ($n = 2, 3, 4$) [17,18] which corresponds to an axially elongated hcp lattice ($c/a \sim 1.8$).

Some rare earth metals (La, Nd, Pr) are known to have an ABCB sequence of

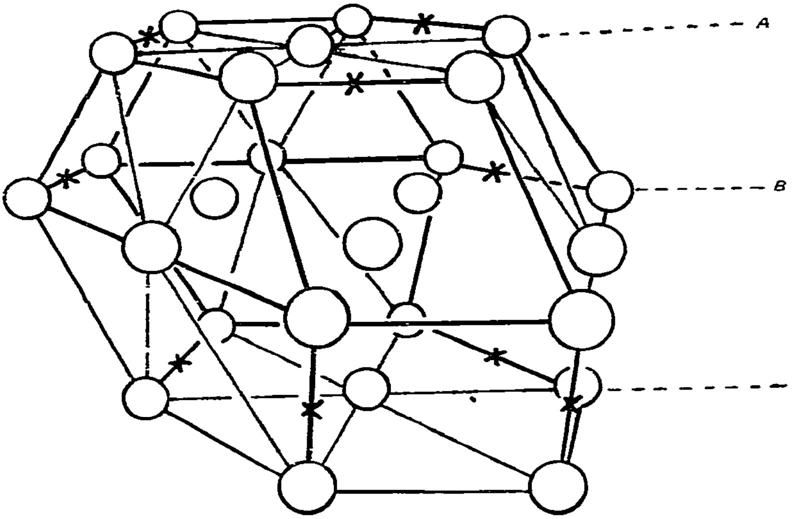

Fig. 2. The metallic skeleton and the corresponding polyhedron with the carbonyl distribution found in the $[Pt_{26}(CO)_{23}(\mu\text{-}CO)_9]^{2-}$ cluster [23]. Each of the 23 external Pt atoms has 1 terminal CO and the edge-bridging CO's are indicated by —×—.

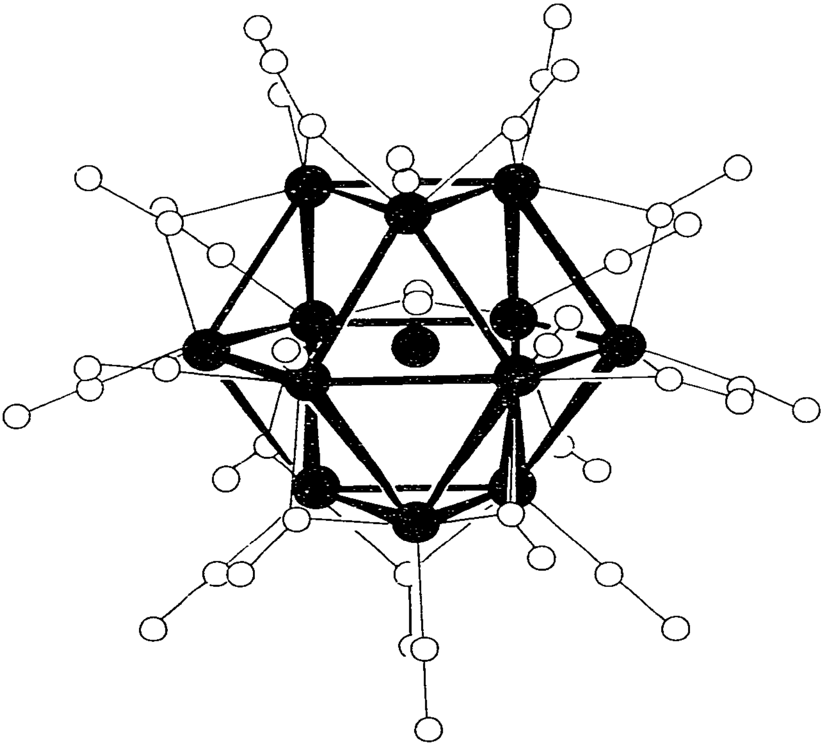

Fig. 3. The molecular structure of the $[Rh_{13}(CO)_{24}H_{5-n}]^{n-}$ anions, n = 2,3,4 [7,8,74a].

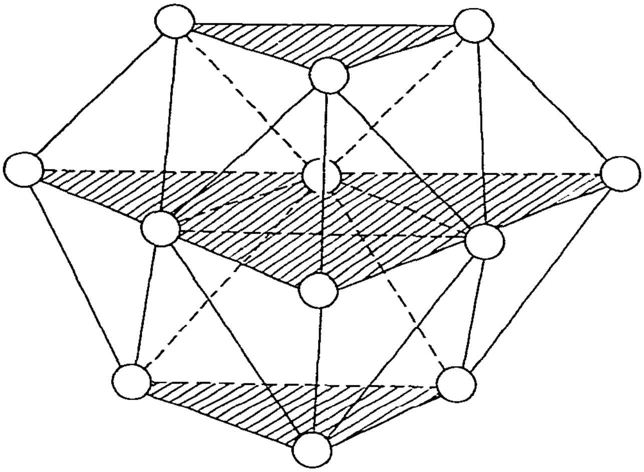

Fig. 4. The metallic skeleton of the $[Ni_{12}(CO)_{21}H_{4-n}]^{n-}$ anions, $n = 2,3,4$ [17,18].

close-packed layers [100] and the cluster $[Rh_{22}(CO)_{37}]^{4-}$, shown in Fig. 5, which may be derived by capping all the square faces of a central twinned cube-octahedron and adding a further layer of three metal atoms, contains the same type of ABCB sequence [74a].

Although the synthesis of large rhodium carbonyl clusters via thermal condensation has not yet been studied at a level comparable to that of the platinum clusters, interconversion between different packings of metal atoms has again been observed. Reactions 6 and 7 transform the hcp $[Rh_{13}(CO)_{24}H]^{4-}$ of Fig. 3 into the bcc $[Rh_{14}(CO)_{25}]^{4-}$ species shown in Fig. 6. Moreover, simple substitution of a double negative charge with one carbonyl to give the species $[Rh_{14}(CO)_{26}]^{2-}$ brings about a new structural change; the structure of this

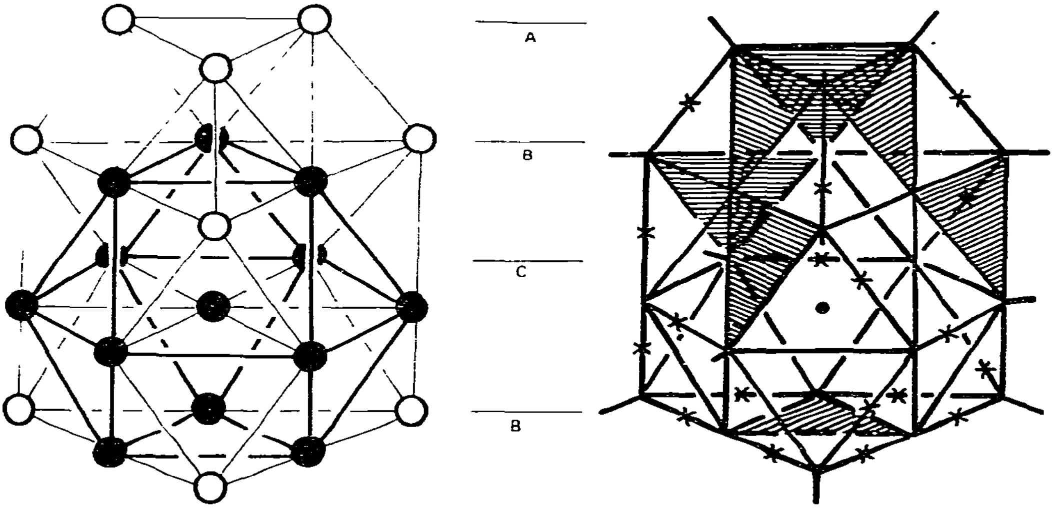

Fig. 5. The metallic skeleton and the distribution of the carbonyls in the cluster $[Rh_{22}(CO)_{12}(\mu\text{-}CO)_{18}\text{-}(\mu_3\text{-}CO)_7]^{4-}$ of C_{3v} symmetry [74a].

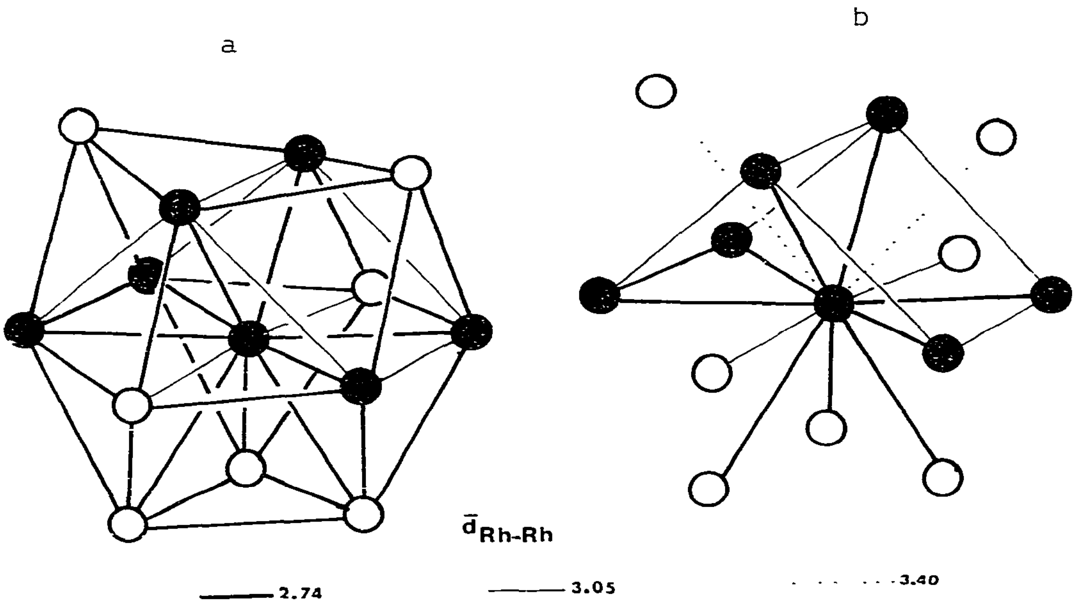

Fig. 6. The metal atom cluster in the $[Rh_{14}(CO)_{25}]^{4-}$ anion with the surface metal—metal bonds (a) and the centre to surface ones (b). Mean standard deviation 0.005 Å [72].

latter compound is intermediate between bcc and close-packing [74a], similar to that previously found in $[Rh_{15}(CO)_{27}]^{3-}$ [72]. As shown for instance in Fig. 7, the seven metal atoms in the horizontal hexagonal plane divides both $[Rh_{14}(CO)_{26}]^{2-}$ and $[Rh_{15}(CO)_{27}]^{3-}$ into two subunits. The upper part is bcc and contains the central metal atom in the centre of an incomplete capped cube, while the lower part is close-packed. The central metal atom gives rise

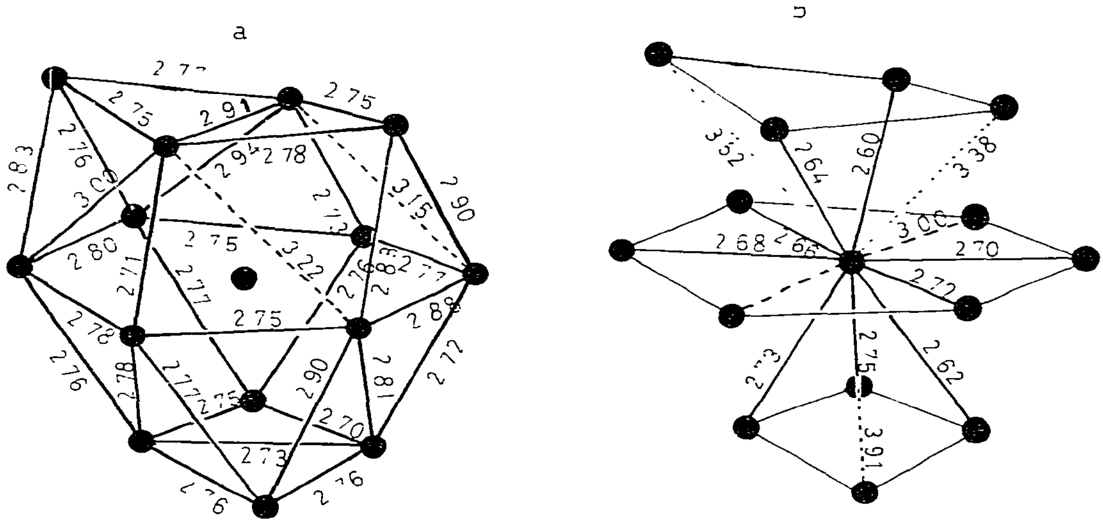

Fig. 7. The metal atom cluster in the $[Rh_{15}(CO)_{27}]^{3-}$ anion with the surface metal—metal bonds (a) and the centre to surface ones (b). Mean standard deviation 0.005 Å [72].

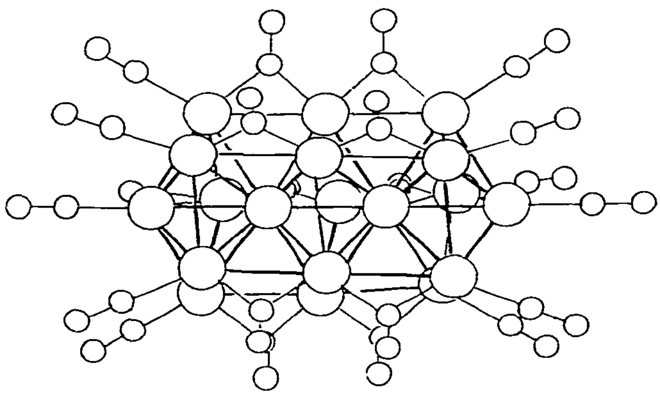

Fig. 8. The schematic D_{5h} structure of the $[Pt_{19}(CO)_{12}(\mu\text{-}CO)_{10}]^{4-}$ cluster. The Pt—Pt average distance in the pentagonal planes is 2.88 Å, while all the other distances average to 2.76 Å [99].

only to eleven short metal—metal bonds. The $[Rh_{14}(CO)_{25}H]^{3-}$ cluster shows a similar intermediate packing in which only ten short metal—metal bonds are present around the central metal atom [74a]. All of these are examples of the increased freedom of arrangements which clusters can adopt.

A common basic structural situation has been found in $[Pt_{19}(CO)_{22}]^{4-}$ [99] and $[Rh_{15}(CO)_{28}(C)_2]^-$ [4]. In both cases the central metal atoms are found in the centre of a pentagonal prism bicapped on both pentagonal bases, Figs. 8 and 9. In a regular pentagonal bicapped prism the height of the prism is 1.05 times the length of the pentagonal sides, and therefore 7 of the 37 metal—metal contacts are increased by 1.05. This situation can be relieved in several ways: one, proposed by Bagley [11], requires an increase of the 10 pentagonal sides to 1.02 and results in a packing efficiency of 73.41%. The structure of the $[Pt_{19}(CO)_{22}]^{4-}$ cluster approximates to this situation [99], and we can now therefore substantiate the hypothesis of Bagley that this type of "pseudolattice' is present in five-fold small metallic crystallites and whiskers. A different

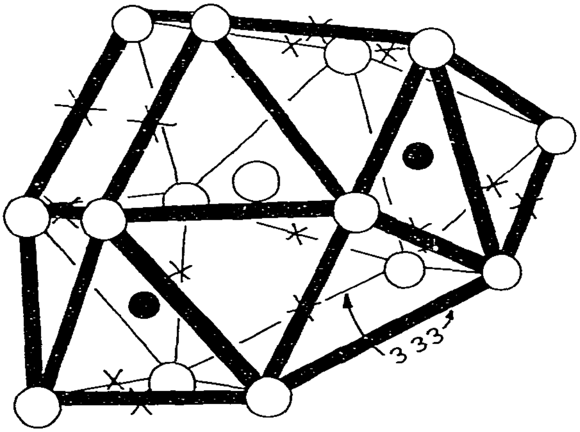

Fig. 9. Schematic C_{2v} structure of the $[Rh_{15}(CO)_{28}(C)_2]^-$ anion. One terminal carbonyl per surface metal atom is present; bridging carbonyls are indicated by crosses and interstitial carbides by ● [4].

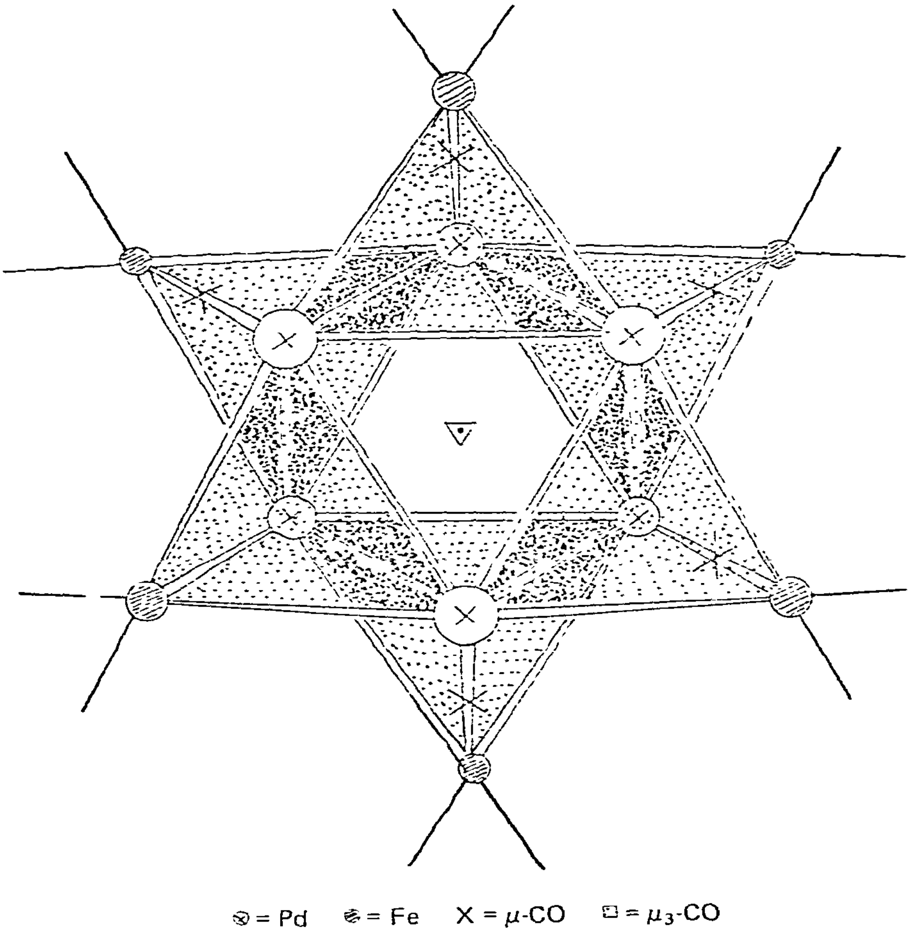

Fig. 10. (a) The metallic skeleton, based on a hexacapped octahedron of idealised D_{3h} symmetry, found in the cluster $[Fe_6Pd_6(CO)_{24}H]^{3-}$ [63].

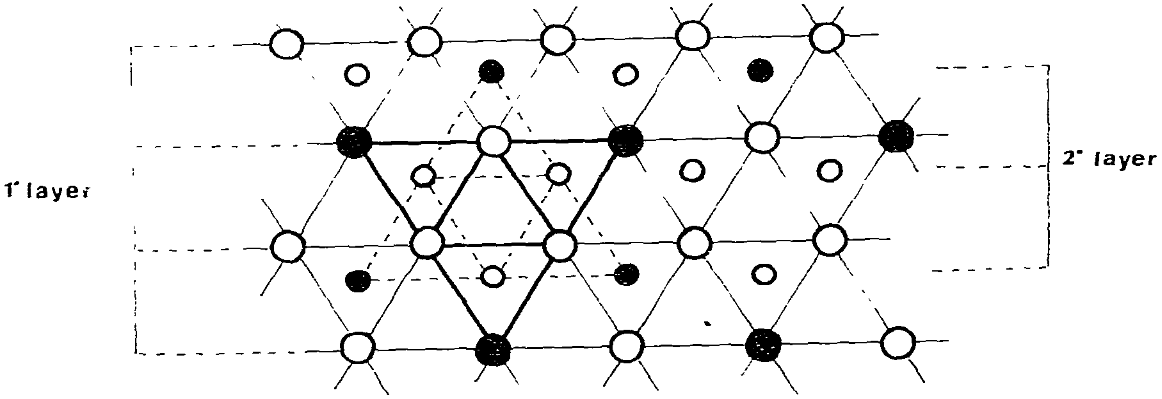

Fig. 10. (b) The corresponding representation of two layers in M'_3M'' alloys such as Cu_3Au (ccp) and Ni_3Sn (hcp) [100].

possibility requires two pentagonal sides to be extended to a value of 1.09, and results in loss of the five-fold axes; this second arrangement is found in $[Rh_{15}(CO)_{28}(C)_2]^-$ [4]. Both of these findings are relevant to classical solid state chemistry.

Finally, the structure of $[Fe_4Pt_6(CO)_{22}]^{2-}$ and $[Fe_6Pd_6(CO)_{24}H]^{3-}$ (Fig. 10a), two clusters which have been prepared and characterised by G. Longoni and M. Manassero [63,64], show that in both cases the iron has a stronger tendency to form metal—carbon monoxide bonds with the precious metal, which prefers to form metal—metal bonds, being in the interior. A comparison of the two limiting possibilities:

$\bar{D}(\text{Fe—CO}) + \bar{D}(\text{Pd—Pd}) > \bar{D}(\text{Pd—CO}) + \bar{D}(\text{Fe—Fe})$

(observed situation) (alternative situation)

or

$\bar{D}(\text{Fe—CO}) - \bar{D}(\text{Fe—Fe}) > \bar{D}(\text{Pd—CO}) - \bar{D}(\text{Pd—Pd})$

indicates once more [27] that the difference $\bar{D}(\text{M—CO}) - \bar{D}(\text{M—M})$ decreases on descending the subgroups. Figure 10 also shows the similarity between the two layers present in $[Fe_6Pd_6(CO)_{24}H]^{3-}$ and the ordered super-structures found in M'_3M'' alloys such as Cu_3Au (ccp) and Ni_3Sn (hcp) [100].

Comparison of LMCC and interstitial alloys

Large hydride clusters may contain the hydrides in octahedral interstitial positions, but, in this case, the metal atoms bound to the hydride usually present a sensible increase of the corresponding metal—metal distances (0.05—0.07 Å). This behaviour indicates a limited possibility of overlap between the system of metal—metal bonds and the totally symmetric *s* orbital of the hydride and the presence of related repulsive effects [29]. Therefore, systematic occupation of interstitial holes is expected only in large clusters in which: a) there is still a sufficient number of empty cavities which can sustain the network of metal—metal bonds [29], and b) the metal coordination numbers of the surface metal atoms are low (typically 5—6) giving rise to limited local disturbance of the metallic skeleton [31]. The first of these conditions is absent in the usual 4—7 metal atom clusters, for example in an octahedron, where occupation of the interstitial hole takes place in $[Co_6(CO)_{15}H]^-$ [45] (but not in $[Rh_6(CO)_{15}H]^-$) [30]; and in $[Ru_6(CO)_{18}H]^-$ [37] (but not in $[Os_6(CO)_{18}H]^-$) [75]. The exceptional interstitial nature of the hydride in these two hexanuclear clusters has not yet been explained, but it is probably related to the steric requirements of the ligands which results in expanded metal—metal distances able to readily accommodate the hydride (see later for a similar synergism between carbide accommodation and paramagnetism).

Neutron diffraction has been used by L.F. Dahl and co-workers to prove the octahedral interstitial situation for the $[Ni_{12}(CO)_{21}H_{4-n}]^{n-}$ ($n = 2, 3$) hydrides [17], and a combination of PMR spectroscopy at low temperature [71] and structural X-ray determinations [7,8,74a] has also shown this to be the case for the $[Rh_{13}(CO)_{24}H_{5-n}]^{n-}$ ($n = 2, 3, 4$) hydrides. Analogous octahedral

TABLE 1

APPARENT RADIUS AND COORDINATION OF THE CARBON ATOM IN INTERSTITIAL CARBIDES [52] AND CARBONYL CLUSTERS [5,6,27]

Coordination		Apparent radius = $d(\mathrm{M—C}) - 1/2\ d(\mathrm{M—M'})$ (Å)
Octahedral	TiC (ccp)	0.63
	W_2C (hcp)	0.67
	$[Fe_6(CO)_{16}C]^{2-}$	0.57
	$Ru_6(CO)_{17}C$	0.61
	$[Rh_{15}(CO)_{28}(C)_2]^-$	0.60
Trigonal prismatic	WC (hex)	0.76
	Fe_3C (orthorhombic)	0.715
	$[Rh_6(CO)_{15}C]^{2-}$	0.74
	$Rh_8(CO)_{19}C$	0.72
	$[Co_{13}(CO)_{24}(C)_2H]^{4-}$	0.69
Square antiprismatic	$Cr_{23}C_6$	0.845
	$[Co_8(CO)_{18}C]^{2-}$	0.81

hole occupation and elongation of metal—metal bonds are known for the binary hydrides of the late transition metals [29].

^1H-$\{^{103}Rh\}$ INDOR NMR spectroscopy shows the interstitial hydrides in the $[Rh_{13}(CO)_{24}H_{5-n}]^{n-}$ ($n = 2, 3$) anions to be completely fluxional at room temperature [71], $\Delta G^{\neq}$ for their migration is about 10 kcal mol^{-1} and k_H/k_D is about 4.6 [46]. This high mobility could be accounted for by involving a temporary protonic character of the hydride during the required jumps through the internal triangular faces of the metallic skeleton, and this charge transfer is not unreasonable in a "quasi" metallic situation where only a small separation between LUMO and HOMO should be present. Moreover it agrees with the observed ready extraction of these hydrides as protons, a reaction which often takes place by simple dissolution in basic solvents such as DMSO [30].

In contrast to interstitial hydrides, interstitial carbides do not usually result in increased metal—metal distances, probably because the carbon *p* orbitals can overlap with MO's of a number of different symmetries [31]. Table 1 compares the apparent radius and the coordination geometry of carbide atoms observed in clusters and in binary carbides. It clearly shows that carbonyl carbide clusters represent an additional point of contact between molecular compounds and infinite lattices; carbide accommodation, as for hydride accommodation, can also take place in the limited metallic frame of a cluster and examples are found for metals (Ru, Os, Rh) where there is no carbide accommodation in the extended metallic lattice. Moreover, structures based on condensed systems of trigonal prismatic cavities are readily recognised both in $[Rh_{12}(CO)_{24}(C)_2]^{2-}$ (Fig. 11) [90] and in $[Co_{13}(CO)_{24}(C)_2H]^{4-}$ (Fig. 12) [6]; both are reminiscent of the well known structure of cementite [40].

The additional stability imparted to the cluster by the carbide atoms can be readily illustrated with the unique example of a stable paramagnetic octahedral cluster ($g = 2.013$) which is readily prepared by the quantitative reaction [9]:

$$[Co_6(CO)_{15}C]^{2-} + Fe^{3+} \xrightarrow{25^\circ\mathrm{C,\ THF}} [Co_6(CO)_{14}C]^- + CO + Fe^{2+} \qquad (14)$$

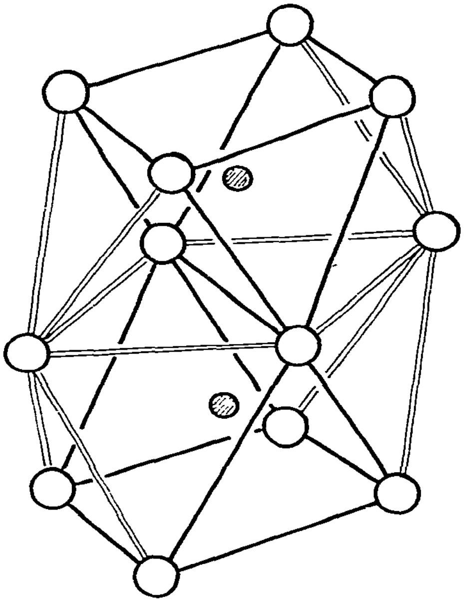

Fig. 11. Schematic D_{2h} structure of $[Rh_{12}(CO)_{16}(\mu\text{-}CO)_8(C)_2]^{2-}$ (the two trigonal prismatic units have been emphasised) [90].

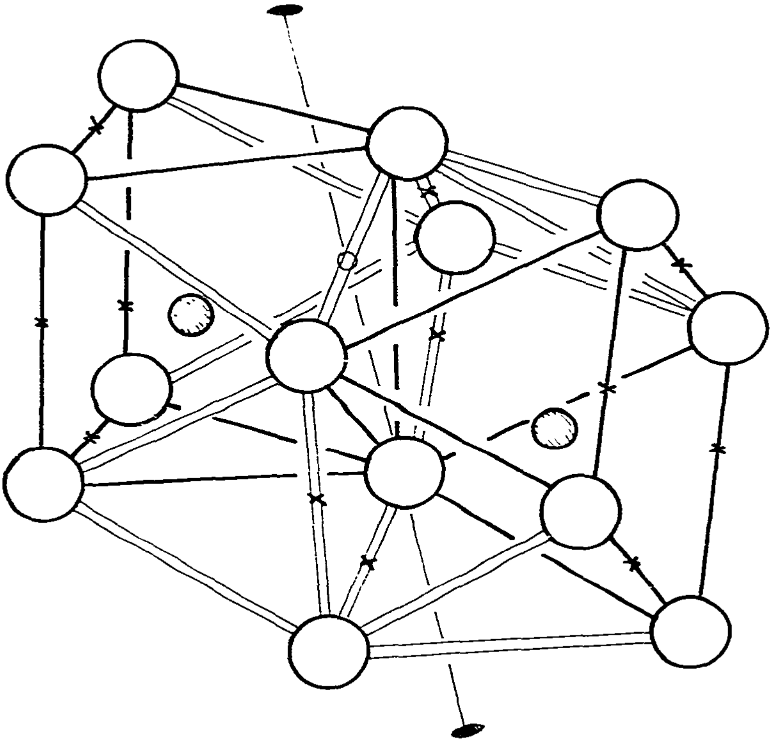

Fig. 12. The $Co_{12}C_2$ core found in the $[Co_{13}(CO)_{12}(\mu\text{-}CO)_{12}(C)_2H]^{4-}$ cluster, the solid lines define the trigonal prismatic moieties [6].

TABLE 2

NMR DATA ON ENCAPSULATED ATOMS

Compound	Encapsulated atom	Geometrical environment	Chemical shift (ppm)	NMR	Ref.
$[Rh_{13}(CO)_{24}H_3]^{2-}$	Rh	Fig. 3	+3547	3.16 MHz	[71]
$[Rh_{13}(CO)_{24}H_2]^{3-}$	Rh	Fig. 3	+4954	3.16 MHz	[71]
$[Rh_{13}(CO)_{24}H]^{4-}$	Rh	Fig. 3	+6370	3.16 MHz	[46]
$[Rh_6(CO)_{13}C]^{2-}$	C	octahedron	+338	TMS	[90]
$[Rh_6(CO)_{15}C]^{2-}$	C	trig. prism	+264	TMS	[3]
$[Co_6(CO)_{15}C]^{2-}$	C	trig. prism	+330.5	TMS	[5]
$[Co_8(CO)_{18}C]^{2-}$	C	square antiprism	+388	TMS	[90]
$[Rh_9(CO)_{21}P]^{2-}$	P	square antiprism	+282.3	(H_3PO_4)	[96]
$[Co_6(CO)_{15}H]^-$	H	octahedron	+23.2	TMS	[45]
$[Ru_6(CO)_{18}H]^-$	H	octahedron	+16.4	TMS	[37]
$[Ni_{12}(CO)_{21}H_2]^{2-}$	H	dist. octahedron	—18	TMS	[17]
$[Ni_{12}(CO)_{21}H]^{3-}$	H	dist. octahedron	—24	TMS	[17]
$[Rh_{13}(CO)_{24}H_3]^{2-}$	H	square pyramid fluxional [a]	—29.3	TMS	[71]
$[Rh_{13}(CO)_{24}H_2]^{3-}$	H	square pyramid fluxional [b]	—26.7	TMS	[71]

[a] At —90°C two signals in the ratio 1 : 2 are observed at —28.3 and —30.8 ppm [30]. [b] At —90°C two signals in the ratio 1 : 1 are observed at —26.9 and —27.8 ppm [46].

In this case the paramagnetism and carbide accommodation are probably synergic effects, because the unpaired electron elongates metal—metal bonds [92] and allows a better accommodation of the carbide atom in the limited space provided by the octahedron of cobalt atoms (and vice versa).

Obviously it should be possible to extend this chemistry to a number of other interstitial elements such as B, N, Si, P and S. Synthetic routes for incorporating boron and silicon atoms have not yet been developed. The $[Rh_9(CO)_{21}P]^{2-}$ and $[Rh_{17}(CO)_{32}(S)_2]^{3-}$ anions based on square antiprismatic holes have been prepared at high pressure and structurally characterised by J. Vidal [95,96], and the anions $[M_6(CO)_{15}N]^-$ (M = Co, Rh), which contain the nitrogen atom in a trigonal prismatic hole, have recently been reported by S. Martinengo [73].

Encapsulated atoms can be used as a sensitive probe of the electronic distribution in large clusters, and most of the available NMR data (Table 2) on encapsulated atoms are consistent in showing resonances at extremely low fields, where cationic forms of these elements are usually found. The exceptional high field position found in several hydrides may be related to an out-of-centre situation of this small atom in the hole, as observed in $[Ni_{12}(CO)_{21}H_{4-n}]^{n-}$ by neutron diffraction ($\bar{d}$(Ni—H) = 1.84 and 2.00 Å when $n = 3$, and 1.72 and 2.22 Å when $n = 2$) [17] and required in the incomplete octahedral cavities of the $[Rh_{13}(CO)_{24}H_{5-n}]^{n-}$ anions. The positive character of the central rhodium atom present in the twinned cube-octahedron shaped $[Rh_{13}(CO)_{24}H_{5-n}]^{n-}$ species is particularly interesting because SCF-Xα-SW calculations on similar cube-octahedral shaped systems of 13 bare metal atoms have found a negative charge on the central metal atom, which is due to the deeper potential well of this atom in the surrounding field of 12 nuclei [76]. The observed charge reversion at the central metal atom is probably induced by the collective effect of the external π-acidic carbonyl groups and transmitted through the high polarisability of the metallic electronic density. Evidence for this situation is found in recent CNDO calculations on $Co_4(CO)_{12}$ which show a positive charge on the metal atoms [41].

The relevance of ligands in LMCC

The present level of structural knowledge of LMCC is summarised in Table 3. This table shows that the ratio between the carbonyl ligands and the metal atoms is the main parameter responsible for the different aggregation of the metal atoms to give loosely coupled systems (vertex connected double polyhedra, Fig. 13, or expanded stacks of triangular units, Fig. 14), or real fragments of tridimensional lattices and pseudolattices. Whereas the presence of internal ligands (interstitial heteroatoms) is obviously dictating the formation of particular structures containing cavities suitable for their accommodation, as found in the solid state, the observed effect of the CO/M ratio deserves some discussion.

Carbon monoxide is one of the smallest ligands and is not usually suspected of producing pronounced steric effects, although the steric stabilisation of the radical carbonyl $V(CO)_6$ has been known for many years. A systematic examination of the shortest interligand distances observed in carbonyl clusters is consistent with the oxygens of parallel carbonyls being in contact at minimum distances of about 2.9—3.05 Å, whereas between carbonyls at a relative angle of around 100° the carbon atoms are in contact at a minimum distance of about 2.5—2.6 Å.

Tetrahedral carbonyl clusters containing more than 13 carbonyls are not known experimentally, and clusters richer in carbon monoxide, such as $[Re_4(CO)_{15}H_4]^{2-}$ and $[Re_4(CO)_{16}]^{2-}$, adopt more open geometries [28]. Similarly, the maximum number of carbonyls found around an octahedron of metal atoms is 18, and even this figure seems only possible with the larger second and

TABLE 3

SUMMARY OF THE STRUCTURAL CHEMISTRY OF LARGE METAL CARBONYL CLUSTERS

Isolated small polyhedra	$[Rh_6(CO)_{14}]^{4-}$		CO/M ≥ 2
Vertex connected double polyhedra	$[Rh_{12}(CO)_{30}]^{2-}$		
Expanded stacks of triangles	$[Pt_{15}(CO)_{30}]^{2-}$		
Lattice- and pseudolattice-related clusters	$[Pt_{38}(CO)_{44?}]^{2-}$	ccp	CO/M < 2
	$[Rh_{13}(CO)_{24}H_{5-n}]^{n-}$	hcp	
	$[Rh_{22}(CO)_{37}]^{4-}$	ABAC	
	$[Rh_{14}(CO)_{25}]^{4-}$	bcc	
	$[Rh_{15}(CO)_{27}]^{3-}$	bcc/cp	
	$[Pt_{19}(CO)_{22}]^{4-}$	5 fold	
Interstitial alloy-related clusters	$[Rh_{12}(CO)_{24}(C)_2]^{2-}$	trig. prism	presence of heteroatoms
	$[Co_8(CO)_{18}C]^{2-}$	square antiprism	
Alloy-like clusters	$[Fe_6Pd_6(CO)_{24}H]^{3-}$		mixed metal atoms

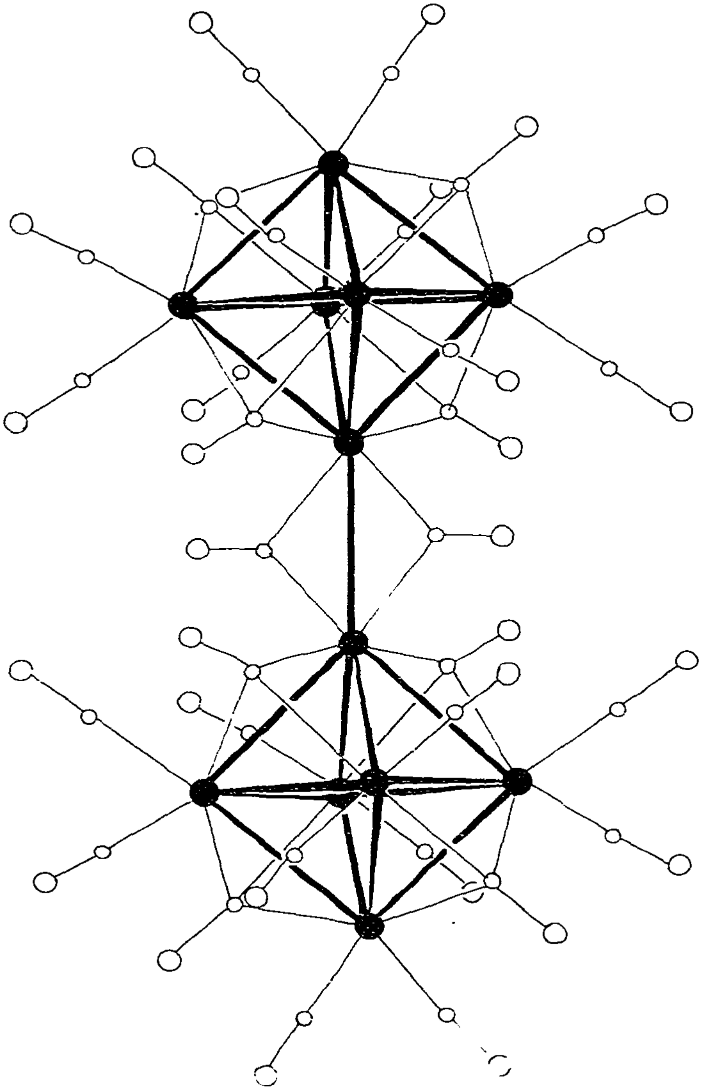

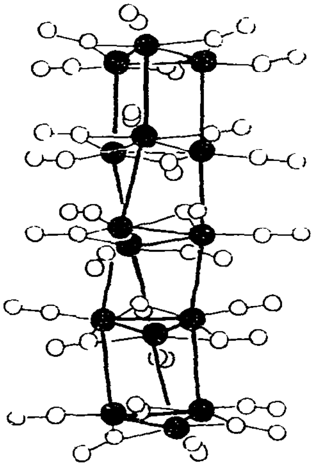

Fig. 13 (left). Schematic C_{2h} structure of $[Rh_{12}(CO)_{30}]^{2-}$ [1].

Fig. 14 (right). Schematic C_3 structure of the $[Pt_{15}(CO)_{30}]^{2-}$ dianion, $\bar{d}$(Pt—Pt) 2.66 Å inlayer and 3.08 Å interlayer [20].

third row transition metals at the expenses of considerable elongation of the metal—metal distances (0.1—0.2 Å). With iron these pronounced steric effects are well illustrated by the stability of the violet radical anion $[Fe_3(CO)_{11}]^-$ ($g = 2.05$) [55], which may be obtained by the redox redistribution [65].

$$Fe_3(CO)_{12} + [Fe_3(CO)_{11}]^{2-} \xrightarrow[THF]{25^\circ C} 2[Fe_3(CO)_{11}]^- + CO \quad (15)$$

This radical anion does not dimerise to the expected $[Fe_6(CO)_{18}]^{2-}$ and can even be isolated in the solid state. Similarly the series of $[M_3(CO)_6]_n{}^{2-}$ anions, exemplified in the structure of $[Pt_{15}(CO)_{30}]^{2-}$ shown in Fig. 14, ends at $n = 3$ for nickel due to the strain imposed by the nonbonding interactions between the parallel carbonyls of the internal layers with Ni—Ni interlayer distances of about 2.8 Å [62].

Moving towards the large polyhedra results in a progressive flattening of the surface, which therefore results both in a decrease of the available space around each carbonyl group and in a more nearly parallel orientation of these ligands. Both these effects operate in the same direction and, as a result, steric crowding becomes dominant in large clusters. Approximate calculations of the maximum number of carbonyls which can be accommodated on polyhedra of increased size have been published [31], and it is well known that in the limiting situation of an extended close-packed surface there is room for only about one carbonyl per metal atom. This steric crowding may be partly alleviated by introducing internal heteroatoms which supply part of the electronic requirement of the cluster. However, this would be sufficient only in borderline cases (Re, Fe, Ru, Os) and will be restricted to structures which present suitable cavities.

In order to allow formation of large clusters it is therefore necessary:

a) to use ligands as small as possible;

b) to use the richest electron metals, thus requiring the minimum possible number of ligands.

The chemistry of large metal carbonyl clusters is concentrated at the end of the transition series only for ligand/steric reasons.

Electron counting in LMCC

The popular analogy between polyhedral boranes and metal carbonyl clusters [98] has a limited value, owing to the requirement that only *s* and *p* orbitals are involved in the cluster bonding. It is based on the fact that in the later transition metals, as a result of the inefficient screening along the transition series, there is considerable contraction of the *d* orbitals and therefore little overlap between these orbitals [77,78]. As a result, most of the *d* band within a cluster has only a small energy spread and in several cases its contribution can even be omitted.

Semiempirical calculations of more general significance have been based on the hypothesis that, due to the different sensitivity to the increasing nuclear charge and to the resulting large separation between $(n-1)d - ns$ and np orbitals which occurs at the end of the transition series, any molecular orbital having energy in substantial excess of the atomic *p* orbitals can be considered antibonding and therefore unavailable for the cluster [57,59]. Using these ideas J.W. Lauher has been able to account for the electronic situation of most of the known clusters and to make predictions for several unknown species [59]. Lauher's numbers can be summarised in the general formula:

$$\text{Number of bonding orbitals} = (N \times 6) + n$$

where the number of bonding orbitals corresponds to half of the cluster valence electrons reported in Table 4, N is the number of metal atoms, and n is the number of extra bonding orbitals which are available, and, as shown in Table 4,

TABLE 4

ELECTRON COUNTING IN THE LARGEST TRANSITION METAL CLUSTERS

N number of metal atoms		Symmetry	Cluster valence electrons	n number of extra bonding orbitals	Ref.
7	$[Rh_7(CO)_{16}]^{3-}$	C_{3v}	98	7	27
	$[Rh_7(CO)_{16}I]^{2-}$	C_{3v}	100	8	27
8	$[Ni_8(CO)_8(PPh)_6]$	O_h	120	12	66
	$[Rh_8(CO)_{19}C]$	C_i	114	9	27
	$[Cu_2Rh_6(CO)_{15}(RCN)_2]$	D_{3h}	110	7	10
9	$[Rh_9(CO)_{21}P]^{2-}$	C_{4v}	130	11	96
	$[Ni_9(CO)_{18}]^{2-}$	C_3	128	5 × 2 [a]	21
10	$[Fe_4Pt_6(CO)_{22}]^{2-}$	S_4	138	9	64
11	$[Au_{11}I_3(PR_3)_7]$	C_{3v}	138	3	14
12	$[Rh_{12}(CO)_{30}]^{2-}$	C_{2h}	170	6.5 × 2 [a]	1
	$[Pt_{12}(CO)_{24}]^{2-}$	C_3	170	4.3 × 3 [a]	21
	$[Ni_{12}(CO)_{21}H_2]^{2-}$	D_{3h}	166	5.5 × 2 [a]	17
	$[Rh_{12}(CO)_{24}(C)_2]^{2-}$	D_{2h}	166	11	4
	$[Rh_{12}(CO)_{25}C_2]$	C_i	166	11	90
	$[Fe_6Pd_6(CO)_{24}H]^{3-}$	D_{3h}	160	8	63
13	$[Co_{13}(CO)_{24}(C)_2H]^{4-}$	C_2	178	11	6
	$[Rh_{13}(CO)_{24}H_3]^{2-}$	D_{3h}	170	7	7
	$[Au_{13}(dppm)_6]^{4+?}$	I_h	163	3.5	97
14	$[Rh_{14}(CO)_{33}(C)_2]^{2-}$	C_{2v}	202	8.5 × 2 [a]	90
	$[Rh_{14}(CO)_{25}]^{4-}$	C_{4v}	180	6	72
	$[Rh_{14}(CO)_{26}]^{2-}$	C_s	180	6	74a
15	$[Pt_{15}(CO)_{30}]^{2-}$	C_3	212	4 × 4 [a]	20
	$[Rh_{15}(CO)_{28}(C)_2]^{-}$	C_{2v}	200	10	4
	$[Rh_{15}(CO)_{27}]^{3-}$	C_1	192	6	72
17	$[Rh_{17}(CO)_{32}(S)_2]^{3-}$	D_{4d}	232	7 × 2 [a] (?)	95
19	$[Pt_{19}(CO)_{22}]^{4-}$	D_{5h}	238	5	99
22	$[Rh_{22}(CO)_{37}]^{4-}$	C_{3v}	276	6	74a
26	$[Pt_{26}(CO)_{32}]^{2-}$	D_{3h}	326	7	23
38	$[Pt_{38}(CO)_{44?}]^{2-}$	O_h	470?	7?	23

[a] Double polyhedron or expanded stack.

is a variable number between 3 and 12. A closer examination shows that n is dependent on the packing of the metal atoms as it increases in the presence of large empty cavities and presents its maximum value in the cube. Exceptionally low values of n (such as 3) are an artefact due to the unavailability of the complete set of p orbitals which arises after the $4f$ filling (Pt, Au), and are sterically relevant to the existence of an exceptional cluster chemistry of these elements. Although the average and most usual figure of n is 7, it has not yet been possible to rationalise the subtle variation of this parameter using neither a topological, nor a symmetry approach [33a]. However, it is enlightening for the electronic situation of large carbonyl clusters to consider that in the limiting case of an infinite lattice n can be neglected and one is left with 6 bonding orbitals per metal atom. Therefore, this is the maximum number of orbitals which can be filled in a metal, and which is formally reached in the metals of Group IIB (Zn, Cd, Hg). This means that large metal carbonyl clusters can be represented as fragments of metals which are filled at the maximum possible electronic level, a situation clearly related to the high π-acidity of the carbonyl ligands and in full agreement with the well known 18 electron rule [26] observed in low nuclearity metal carbonyl compounds. We can therefore conclude this section by saying that generally electron counting in metal carbonyl clusters will give a figure between the two limiting cases of 18 (low nuclearity metal carbonyls) and 12 (electron saturated infinite metallic lattices) valence electrons per metal atom.

Reactivity of LMCC

Reduction and oxidation reactions of large metal carbonyl clusters are the types of reactions more widely studied owing to their preparative significance; as discussed previously in detail [27], they usually result in substitution of carbon monoxide with a double negative charge and vice versa. Exceptional types of reactions are observed only in the presence of exceptional structural features. For instance ^{195}Pt NMR has shown that intermolecular exchange of triangular units takes place readily in the dianions $[Pt_{12}(CO)_{24}]^{2-}$ and $[Pt_{15}(CO)_{30}]^{2-}$ (Fig. 14) owing to steric hindrance between the internal units [19]. The coordinatively unsaturated fragment $Pt_3(CO)_6$ involved in this exchange is probably responsible for the exceptional ease of reduction of both these species by molecular hydrogen [61], for instance:

$$3[Pt_{12}(CO)_{24}]^{2-} + H_2 + H_2O \xrightleftharpoons{25^\circ C,\ THF,\ 1\ atm} 4[Pt_9(CO)_{18}]^{2-} + 2\,H_3O^+ \qquad (16)$$

Similarly, the dianion $[Rh_{12}(CO)_{30}]^{2-}$ in Fig. 13, which contains a particular intercluster Rh—Rh bond not reinforced by the presence of other metallic components in the same direction, oxidatively adds molecular hydrogen according to [30]:

$$[Rh_{12}(CO)_{30}]^{2-} + H_2 \xrightleftharpoons{25^\circ C,\ 1\ atm} 2[Rh_6(CO)_{15}H]^- \qquad (17)$$

Finally, the unusual reduction of $Os_6(CO)_{18}$ by iodide [53]:

$$\underset{\text{(bicapped tetrahedron)}}{Os_6(CO)_{18}} + 3\,I^- \rightleftharpoons \underset{\text{(octahedron)}}{[Os_6(CO)_{18}]^{2-}} + I_3^- \qquad (18)$$

is probably related to the limited stability of its unique arrangement (bicapped tetrahedron) of metal atoms.

It is well known that substitution of carbon monoxide by other ligands may take place with reorganisation of the metallic skeleton, A simple typical reaction being [28]:

$$\underset{\text{(tetrahedron)}}{Co_4(CO)_{12}} + RC{\equiv}CR \rightarrow \underset{\text{("butterfly")}}{Co_4(CO)_{10}(RC{\equiv}CR)} + 2\,CO \qquad (19)$$

Related reactions in which a reversible skeletal change has been observed are:

$$\underset{\text{(tetrahedron) [36]}}{[Fe_4(CO)_{13}]^{2-}} + H^+ \xrightleftharpoons[25^\circ C,\ DMSO]{25^\circ C,\ THF} \underset{\text{("butterfly") [69]}}{[Fe_4(CO)_{13}H]^-} \qquad (20)$$

$$Os_6(CO)_{18}H_2 \underset{CH_2Cl_2}{\overset{THF}{\rightleftarrows}} [Os_6(CO)_{18}H]^- + H^+ \tag{21}$$

(capped square pyramid) [75]
(octahedron) [75]

$$[Rh_{14}(CO)_{25}]^{4-} + H^+ \underset{DMSO,\ Na_2CO_3}{\overset{CH_3CN}{\rightleftarrows}} [Rh_{14}(CO)_{25}H]^{3-} \tag{22}$$

(bbc Fig. 6) [72]
(bcc-ccp) [74a]

$$[Rh_6(CO)_{13}C]^{2-} + 2\ CO \underset{60^\circ C,\ N_2}{\overset{25^\circ C,\ 1\ atm}{\rightleftarrows}} [Rh_6(CO)_{15}C]^{2-} \tag{23}$$

(octahedron) [90]
(trigonal prism) [2]

$$[Rh_4Pt(CO)_{12}]^{2-} + 2\ CO \underset{25^\circ C,\ N_2}{\overset{25^\circ C,\ 1\ atm}{\rightleftarrows}} [Rh_4Pt(CO)_{14}]^{2-} \tag{24}$$

(trigonal bipyramid, Pt axial) [43]
(trigonal bipyramid, Pt equatorial) [43]

Again, in most of these examples particular structural features responsible for the remarkable ease of interconversion may be identified, and it is relevant that a similar migration of metal atoms is known in surface chemistry. This was originally observed while studying the surface composition of alloys in the presence of different chemisorbed ligands [86]; more recently a similar reorganisation has been observed on extended monometallic surfaces and this is now known as ligand induced surface reconstruction [16,68,94].

Complete or partial fluxionality of the carbonyls is usual in cluster chemistry and has been recently reviewed [13,39]. There is little doubt that complete fluxionality is related to the possibility of different distributions of the carbonyls as recently discussed in detail for icosahedral-cuboctahedral interconversion of the arrangement of the ligands in $M_4(CO)_{12-x}L_x$ clusters [54]. Migration of ligands on extended surfaces is probably dependent on the coverage, and it has been pointed out that the two processes are only superficially similar [80].

Catalysis via LMCC

Clusters have been used, at least since 1964 as catalysts [12], and a recent review [89] shows that clusters can be applied to several processes such as oxidation, oligomerisation, polymerisation, hydrogenation and hydroformylation. We have ourselves used $[Ni_{12}(CO)_{21}H_2]^{2-}$ to transform acetylene into polyacetylene (acetone, 25°C, 1 atm) [22], $Rh_8(CO)_{19}C$ to polymerise THF into solid polymers (25°C) [90], and $[Rh_{13}(CO)_{24}H_{5-n}]^{n-}$ ($n = 2, 3$) to hydrogenate olefins (acetone or THF, 25°C, 1 atm) [30]. Here we must accept that a catalyst is an agent which makes the reaction proceed regardless of whatever transformation it may undergo. If we restrict this definition, and ask whether the catalytically active species is an intact cluster, the picture becomes much more foggy. Direct evidence of authentic cluster catalysis by structural characterisation of at least some of the reactive intermediates involved in the catalytic cycle is a rather difficult task. However, the recent X-ray characterisation (Fig.

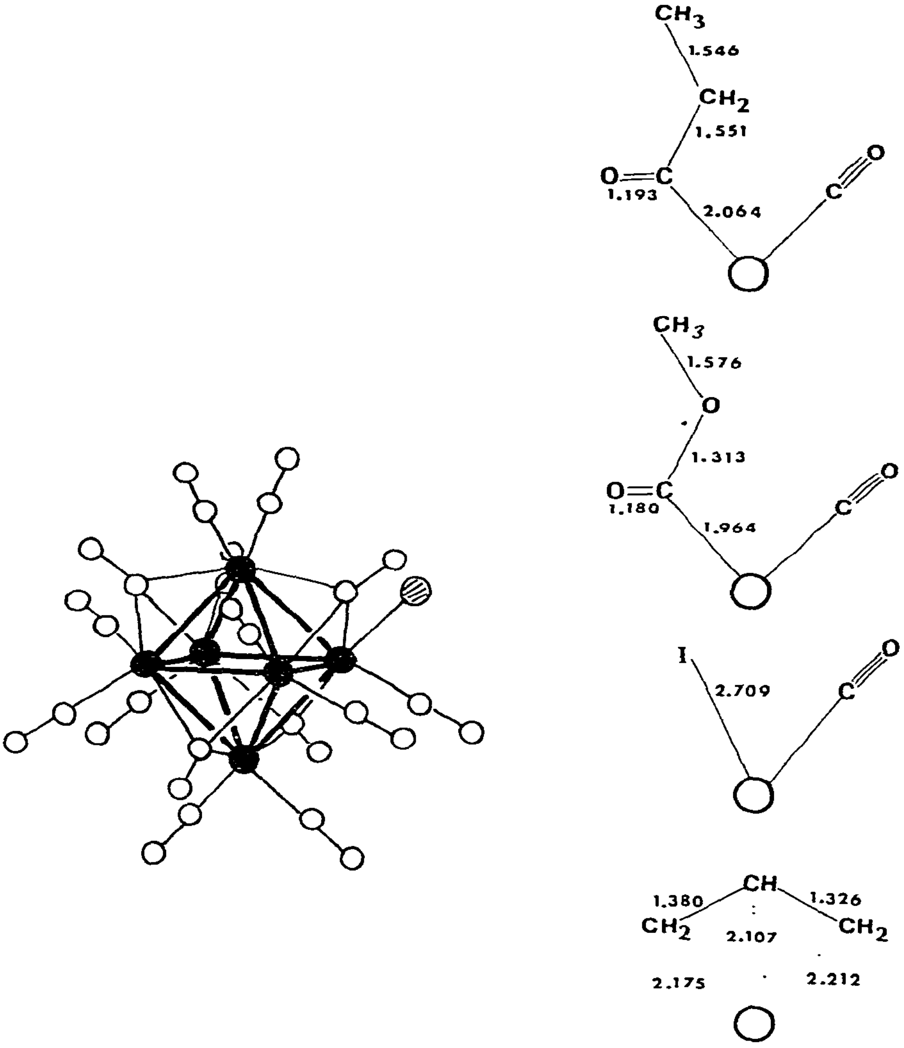

Fig. 15. Structural data on $[Rh_6(CO)_{14}(\eta^3\text{-}C_3H_5)]^-$ and on $[Rh_6(CO)_{15}X]^-$ (X = COEt, COOMe) anions [33b,c].

15) of the alkyl, acyl and carboalkoxy anions $[Rh_6(CO)_{14}(\eta^3\text{-}C_3H_5)]^-$ and $[Rh_6(CO)_{15}X]^-$ (X = COEt, COOMe) [33b,c], and the PMR characterisation of the corresponding hydride $[Rh_6(CO)_{15}H]^-$ [30] provide reasonable evidence for the assumption that clusters can at least carry the functional groups required in a catalytic reaction. Actually, not only the hydride adds olefins to give acyl derivatives [74b], but moreover the presence of $[Rh_6(CO)_{15}X]^-$ species has been observed in the catalytic hydroformylation of olefins in alkaline conditions [56].

A major problem in cluster catalysis arises from the limited number (4 to 6) and low energy (~20—35 kcal mol^{-1}) of the metal—metal bonds and from the associated ready opening and closing of these bonds. The result is that it may be difficult to define exactly even the number and types of cluster species present under catalytic conditions, and moreover, unless only one of these species is catalytically active, a limited selectivity may arise.

Finally, although the system of ligands and the dispersion of the cluster species present under homogeneous conditions may be considerably different from the corresponding small metallic particles under heterogeneous conditions, in principle, we expect a similar potential catalytic behaviour related to the common ability to:
a) bond the substrate through multicentre bonds [79],
b) provide quasi-synchronous multielectron [88] or multihydride transfer [30],
c) activate potential interstitial atoms.
Therefore a careful comparison of the homogeneous and heterogeneous approaches is required. Actually, both clusters and simple metal carbonyls are useful precursors for the systematic screening of small metallic crystallites dispersed on different carriers. The extreme carrier effect which has been observed in these heterogeneous catalysts open a number of new synthetic possibilities [49,50], and, in the case of the more basic carriers, may indicate the presence of finite clusters even in heterogeneous catalytic conditions [51].

LMCC as models of small metallic crystallites

Growing evidence has been reported in the last few years about the complex nature of metals highly dispersed on carriers. It now seems that in limiting cases completely different situations are possible, going from metallic cations strongly interacting with the surface of the carrier [91], to raft-like aggregates of uncharacterised oxidation state [101], and finally to real tridimensional metallic particles of variable size. In the last case, direct information on the small metallic particles in the range 5—30 Å, which are technically relevant, is mainly limited to size dispersion studies both by high resolution electron microscopy and by chemisorption; large clusters therefore provide a unique opportunity for extrapolating information to these particular systems. However, one should, because of the considerable "size effect" present even in this restricted area, pay particular attention to comparing systems of similar dimension. This is due to the high rate of variation of the average number of surface metal—metal bonds (about from 3 to 7.5) in this range (5—30 Å) and to the expected related variation in the state of the surface metal atoms from a dynamic semiliquid to a nearly rigid solid. Finally any information from LMCC is clearly limited to related situations of high coverage of the chemisorbed ligands giving rise to electronically saturated small metallic particles, and moreover does not take in account a whole range of possible interactions between the particle and the carrier. With these limitations in mind we can now point out the information which can be reasonably extrapolated from the chemistry of large metal carbonyl clusters.
a) Coordination chemistry is expected to provide suitable models for chemisorption [93] at high coverage. However, no extrapolation of the bonding parameters of the carbonyl groups present in large metal carbonyl clusters is yet possible, because these data are probably levelled out by the dominant presence of negative charges.
b) The structural chemistry of LMCC suggest that both the nuclearity and the

packing of metal atoms are dynamic variables dependent on the collective effect of the external and internal ligands. Although in solution both intra- and intermolecular mobilities are easier, we should expect at least intramolecular mobility to be possible and similar in small metallic crystallites. Therefore chemisorption of different ligands is expected to give rise to different arrangements of the metal atoms and to different surfaces. Particularly for very small particles the type and number of active centres are therefore expected to change according to the real operative conditions.

c) There is now good evidence from the structures of $[Pt_{19}(CO)_{22}]^{4-}$ and $[Rh_{15}(CO)_{28}(C)_2]^-$ that the five-fold pseudo-lattices proposed by Bagley [11] are real. Moreover, considering the low efficiency and the longer bonding distances required by the icosahedral packing [67], it now seems reasonable to assume that the known five-fold small metallic crystallites follow the same pseudo-lattice pattern.

d) The accommodation of interstitial hydrides in large clusters is related to the deformation of the metallic skeleton and therefore to a low average number of metal—metal bonds. Small metallic crystallites, but not extended close-packed surfaces, are expected to present a related capability of accommodating interstitial hydrides. Due to the high mobility of the hydride atoms beneath the surface, these systems may present peculiar catalytic properties, for instance they may provide several hydride atoms at the same reaction site of the surface in a quasi-synchronous way [30].

e) In cluster chemistry the ready deformation of the metallic skeleton is also responsible for the accommodation of other heteroatoms, even in cases in which formation of interstitial binary alloys (carbides or nitrides) does not take place in the extended metallic lattices, A similar formation of nitrides is known to be relevant to the Haber process [16] and recent work indicates that superficial (overlayer) carbides are responsible for the hydrocarbon fraction which is formed in the Fischer-Tropsch type of syntheses [83,85]. Generally, systems based on small metallic particles should be able to activate all kind of atoms which can be accommodated in superficial interstitial positions.

Acknowledgements

In this paper I have tried to summarize the joint efforts of several groups: B.T. Heaton at the University of Kent (England) has provided the necessary background for all the NMR work, L.F. Dahl at the University of Wisconsin (USA) and V.G. Albano, presently at the University of Bologna (Italy), have continuously provided most of the effort required for elucidating the solid state structures. I must also mention that some of the more recent preparative results are due to independent work of both G. Longoni and S. Martinengo. Finally I wish to acknowledge financial assistance from CNR (Italy) and from NATO.

References

1 V.G. Albano and P.L. Bellon, J. Organometal. Chem., 19 (1969) 405.
2 V.G. Albano, M. Sansoni, P. Chini and S. Martinengo, J. Chem. Soc., Dalton, (1973) 651.

3 V.G. Albano, P. Chini, S. Martinengo, D.J.A. McCaffrey, D. Strumolo and B.T. Heaton, J. Amer. Chem. Soc., 96 (1974) 8106.
4 V.G. Albano, P. Chini, S. Martinengo, M. Sansoni and D. Strumolo, J. Chem. Soc., Dalton, (1976) 970.
5 V.G. Albano, P. Chini, G. Ciani, M. Sansoni, D. Strumolo, B.T. Heaton and S. Martinengo, J. Amer. Chem. Soc., 98 (1976) 5027.
6 V.G. Albano, S. Martinengo, D. Braga, P. Chini and G. Ciani, XI Ital. Cong. Inorg. Chem., Arcavacata, Sept. 25—29 1978, F-4.
7 V.G. Albano, A. Ceriotti, P. Chini, G. Ciani, S. Martinengo and M. Anker, J. Chem. Soc. Chem. Commun., (1975) 859.
8 V.G. Albano, G. Ciani, S. Martinengo and S. Sironi, J. Chem. Soc., Dalton (1979) 978.
9 V.G. Albano, P. Chini, G. Ciani, M. Sansoni and S. Martinengo, J. Chem. Soc., Dalton, (1980) 163.
10 V.G. Albano, D. Braga, S. Martinengo, P. Chini, M. Sansoni and D. Strumolo, J. Chem. Soc., Dalton, (1980) 52.
11 B. Bagley, Nature, 225 (1970) 1040.
12 C.H. Bamford, G.C. Eastmond and W.R. Maltman, Trans. Faraday Soc., 60 (1964) 1432;
13 E. Band and E.L. Muetterties, Chem. Rev., 78 (1978) 639.
14 P.L. Bellon, M. Manassero and M. Sansoni, J. Chem. Soc., Dalton, (1972) 1481.
15 G. Booth and J. Chatt, J. Chem. Soc., A, (1969) 2131.
16 F. Boszo, G. Ertl, M. Grunz and M. Weiss, J. Catal., 49 (1977) 18.
17 R.W. Broach, L.F. Dahl, G. Longoni, P. Chini, A.J. Schultz and J.M. Williams, Adv. Chem. Ser., 167 (1978) 93.
18 R.W. Broach, L.D. Lower, Trinh-Toan, L.F. Dahl, G. Longoni, A. Cavalieri, M. Manassero, M. Sansoni, and P. Chini, J. Amer. Chem. Soc., in press.
19 C. Brown, B.T. Heaton, A.D.C. Towl, G. Longoni, A. Fumagalli and P. Chini, J. Organometal. Chem., 18 (1979) 233.
20 J.C. Calabrese, L.F. Dahl, P. Chini, G. Longoni and S. Martinengo, J. Amer. Chem. Soc., 96 (1974) 2614.
21 J.C. Calabrese, L. Lower, L.F. Dahl, P. Chini and G. Longoni, unpublished results.
22 A. Ceriotti, G. Longoni and P. Chini, J. Organometal. Chem., 174 (1979) C27.
23 A. Ceriotti, D. Washecheck, L.F. Dahl, G. Longoni and P. Chini, unpublished results.
24 P. Chini, XVIII IUPAC Congress, Munich 1959, Verlag Chemie, A-1, 23.
25 P. Chini, L. Colli and M. Peraldo, Gazz. Chim. Ital., 90 (1960) 1005.
26 P. Chini, Inorg. Chim. Acta Rev., 2 (1968) 31.
27 P. Chini, G. Longoni and V.G. Albano, Adv. Organometal. Chem., 14 (1976) 285.
28 P. Chini and B.T. Heaton, Topics in Curr. Chem., 71 (1977) 1, and references therein.
29 P. Chini, G. Longoni, S. Martinengo and A. Ceriotti, Adv. Chem. Ser., 167 (1978) 1, and references therein.
30 P. Chini, G. Longoni and S. Martinengo, Chim. e Ind. (Milano), 60 (1978) 989.
31 P. Chini, Gazz. Chim. Ital., 109 (1979) 225.
32 P. Chini, G. Ciani, S. Martinengo, A. Sironi, L. Longhetti and B.T. Heaton, J. Chem. Soc., Chem. Commun., (1979) 188.
33 (a) G. Ciani and A. Sironi, J. Organometal. Chem., 197 (1980) 233;
(b) G. Ciani, S. Sironi, P. Chini, A. Ceriotti and S. Martinengo, J. Organometal. Chem., 192 (1980) C39
(c) G. Ciani, A. Sironi, S. Martinengo and P. Chini, unpublished results.
34 J.A. Connor, Topics in Curr. Chem., 71 (1977) 71.
35 P. Costa, Thesis work, University of Milano, 1968.
36 J. Doedens and L.F. Dahl, J. Amer. Chem. Soc., 88 (1966) 4847.
37 C.R. Eady, B.F. Johnson, J. Lewis, M.C. Malatesta, P. Machin and M. McPartlin, J. Chem. Soc. Chem. Commun., (1976) 945.
38 C.R. Eady, B.F. Johnson and J. Lewis, J. Chem. Soc. Chem. Commun., (1976) 302.
39 J. Evans, Adv. Organometal. Chem., 16 (1977) 319.
40 E.J. Fasiska and G.A. Jeffrey, Acta Cryst., 19 (1965) 463.
41 H.J. Freund and G. Hohlneicher, Theoret. Chim. Acta (Berl.), 51 (1979) 145.
42 A. Fumagalli, T.F. Koetzle, F. Tagusagawa, P. Chini, S. Martinengo and B.T. Heaton, J. Amer. Chem. Soc., 102 (1980) 1740.
43 A. Fumagalli, A. Albinati, S. Brukner, B.T. Heaton, S. Martinengo and P. Chini, unpublished results.
44 H. Hagemeyer and D. Hull, U.S. Pat., 2.964.734 (22.4.1948).
45 D.W. Hart, R.G. Teller, C. Wei, R. Bau, G. Longoni, S. Campanella, P. Chini and T.F. Koetzle, Angew. Chem. Int. Ed., 18 (1979) 80.
46 B.T. Heaton, B.E. Mann, S. Martinengo and P. Chini, unpublished results.
47 W. Hieber and J. Ellermann, Z. Naturforsch., B, 18 (1963) 595, and references therein.
48 W. Hieber and E.H. Schubert, Z. Anorg. Allg. Chem., 338 (1965) 32.
49 M. Ichikawa, Bull. Chem. Soc. Japan, 51 (1978) 2268.

50 M. Ichikawa, Bull. Chem. Soc. Japan, 51 (1978) 2273.
51 M. Ichikawa, J. Catal., 59 (1979) 67.
52 Jeitaschko, MTP Int. Rev. Sci. Inorg. Chem., Ser. II, vol. 5, Butterworths, London, 1974, 219, and references therein.
53 G.R. John, B.F. Johnson, J. Lewis and A.L. Mann, J. Organometal. Chem., 171 (1979) C9.
54 B.F. Johnson and R.E. Benfield, J. Chem. Soc., Dalton, (1978) 1554.
55 P.J. Krusic, J. San Filippo, B. Hutchinson, R.L. Nance and L.M. Daniels, J. Amer. Chem. Soc., in press.
56 R.M. Laine, J. Amer. Chem. Soc., 100 (1978) 6451.
57 J.W. Lauher, J. Amer. Chem. Soc., 101 (1979) 2640.
58 J.W. Lauher, personal communication.
59 J.W. Lauher, J. Amer. Chem. Soc., 100 (1978) 5305.
60 G. Longoni, Thesis work, University of Milano, 1967.
61 G. Longoni and P. Chini, J. Amer. Chem. Soc., 98 (1976) 7225.
62 G. Longoni and P. Chini, Inorg. Chem., 15 (1976) 3029.
63 G. Longoni, M. Manassero and M. Sansoni, J. Amer. Chem. Soc., 102 (1980) 3242.
64 G. Longoni, M. Manassero and M. Sansoni, personal communication.
65 G. Longoni and P. Chini, unpublished results.
66 L.D. Lower and L.F. Dahl, J. Amer. Chem. Soc., 98 (1976) 5046.
67 A.L. MacKay, Acta Cryst., 15 (1962) 916.
68 G. Maire, P. Beruhardt, P. Legare and G. Lindauer, Proc. III Int. Conf. Solid Surf., Vienna 1977, 861.
69 M. Manasserro, M. Sansoni and G. Longoni, J. Chem. Soc. Chem. Commun., (1976) 919.
70 S. Martinengo and P. Chini, Gazz. Chim. Ital., 102 (1972) 344.
71 S. Martinengo, B.T. Heaton, R.J. Goodfellow and P. Chini, J. Chem. Soc. Chem. Commun., (1977) 39.
72 S. Martinengo, G. Ciani, A. Sironi and P. Chini, J. Amer. Chem. Soc., 100 (1978) 7096.
73 S. Martinengo, G. Ciani, A. Sironi, B.T. Heaton and J. Mason, J. Amer. Chem. Soc., 101 (1979) 7095.
74 (a) S. Martinengo, G. Ciani and A. Sironi, J. Amer. Chem. Soc., in press;
(b) G. Ciani, A. Sironi and S. Martinengo, J. Organometal. Chem., 192 (1980) C46.
75 M. McPartlin, C.R. Eady, B.F. Johnson and J. Lewis, J. Chem. Soc. Chem. Commun., (1976) 883.
76 R.P. Messmer, S.K. Knudson, K.H. Johnson, J.B. Diamond and C.Y. Yang, Phys. Rev., B, 13 (1976) 1396.
77 D.M.P. Mingos, J. Chem. Soc., Dalton, (1974) 133.
78 D.M.P. Mingos, J. Chem. Soc., Dalton, (1976) 1163.
79 E.L. Muetterties, Bull. Soc. Chim. Belg., 85 (1976) 451, and references therein.
80 E.L. Muetterties, T.L. Rhodin, E. Band, C.F. Brucker and W.R. Pretzer, Chem. Rev., 79 (1979) 91.
81 G. Natta, R. Ercoli and S. Castellano, Atti XLV Riunione Societa Italiana Progresso Scienze, Napoli, October 16—20, 1954.
82 P. Pino and F. Piacenti, in Organic Synthesis via Metal Carbonyls, Ed. I. Wender and P. Pino, vol. II, Wiley 1977, 43.
83 M.L. Poutsma, L.F. Elek., P.A. Ibarbia, A.P. Risch and J.A. Rabo, J. Catal., 53 (1978) 157.
84 A. Quarta, Thesis work, University of Milano, 1967 and S. Martinengo.
85 G.B. Raupp and W.N. Delgass, J. Catal., 58 (1979) 361.
86 W.M.H. Sachtler and R.A. Van Santen, Surface Science, 3 (1979) 121.
87 H. Schafer and H. Schnering, Angew. Chem., 76 (1964) 833.
88 A.E. Shilov, Abstracts XVII ICCC, Hamburg 1976, 181.
89 A.K. Smith and J.M. Basset, J. Molec. Catal., 2 (1977) 229.
90 D. Strumolo, D. Braga, V.G. Albano, S. Martinengo, B.T. Heaton and P. Chini, unpublished results.
91 S.J. Tauster, Fung, S.C. and R.L. Garten, J. Amer. Chem. Soc., 100 (1978) 170.
92 Trinh-Toan, Felhammer W.P. and L.F. Dahl, J. Amer. Chem. Soc., 94 (1972) 3389.
93 R. Ugo, Cat. Rev. Sci. Eng., 11 (1975) 11.
94 M.A. van Hove, in T.N. Rhodin and G. Ertl, "The Nature of the Surface Chemical Bond", North-Holland, 1979, 297.
95 J.L. Vidal, R.A. Fiato, L .. Cosby and R.L. Pruett, Inorg. Chem., 17 (1978) 2574.
96 J.L. Vidal, W.E. Walker, R.L. Pruett and R.C. Schoening, Inorg. Chem., 18 (1979) 129.
97 F.A. Vollenbroek, Thesis, University of Nijmegen 1979.
98 K. Wade, Adv. Inorg. Chem. Radiochem., 18 (1976) 1.
99 D.M. Washecheck, E.J. Wucherer, L.F. Dahl, A. Ceriotti, G. Longoni, M. Manassero, M. Sansoni and P. Chini, J. Amer. Chem. Soc., 101 (1979) 6110.
100 A.F. Wells, Structural Inorganic Chemistry, Clarendon Press, Oxford, IV Ed., 1975, 1018.
101 D.J.C. Yates, L.L. Murrell and E.B. Prestridge, J. Catal., 57 (1979) 41 and references therein.